

Dislocations and faults in some alloys containing copper and aluminium

G. B. MITRA, ANIT K. GIRI

C.S.S. Department, Indian Association for the Cultivation of Science, Jadavpur, Calcutta 700 032, India

By using the method of variance of the respective X-ray diffraction line profile, the effective particle size (p) and r.m.s. strain ($\langle S^2 \rangle^{1/2}$) of four alloys containing copper and aluminium (Al-0.08, 4 and 10 wt% Cu and Cu-5.87 wt% Al) at different annealing stages (starting from the cold filed stages) have been determined. From the peak shift of these samples, their average stacking fault probability $\alpha = \alpha' - \alpha''$ where α' is the intrinsic stacking fault probability and α'' the corresponding extrinsic stacking fault probability, respectively, were determined. Similarly, from the angular distance between the peak and the centroid of the diffraction profiles, the magnitude of $\beta + 4.5\alpha''$, where β is the twinning fault probability, was measured. From these, the true particle size T , the stacking and twinning fault probabilities α' , α'' and β and the minimum stacking fault width D_{\min} have been determined. The hardness of alloys at different annealing stages was found to be dependent on the dislocation density and the stored energy in the alloys. The relation $T \langle S^2 \rangle^{1/2} = \text{constant}$ was found to be valid for the alloys and from this a mechanism of grain growth with annealing has been suggested. With annealing the dislocation density and stored energy per unit volume were found to decrease until finally, in the fully annealed stages, they disappeared. The same was found to be valid for stacking and twinning fault probabilities as well as the minimum stacking fault width. A mechanism for the creation and annihilation of the intrinsic and extrinsic stacking faults has been suggested.

1. Introduction

Dislocations and faults in alloys containing copper and aluminium have aroused much recent renewed interest. Wang and Yu [1] have determined the defect parameters like particle size, strain, and stacking and twinning fault probabilities in the alloys Cu-11.1 and 8.3 at% Al by the X-ray diffraction line profile (XRDL) technique. At the aluminium end of the composition, the alloy Al-4 wt% Cu has been studied in its single-crystal form by Sato *et al.* [2] using the electron microscopic method. There does not appear to be any XRDL study on this alloy although Guinier [3] and Preston [4] have studied these by the single-crystal X-ray method. Preston [4] showed that above 200°C, the copper atoms segregate in localized areas and CuAl₂ cells are formed in between the aluminium cells. While normally the CuAl₂ cells are tetragonal inside the aluminium cells, they get disturbed and tend to adopt a fluorite structure – thus causing the stored energy to be rather high, tending towards contributing high strain hardening. Later Thomas and Washburn [5] showed by electron microscopic studies that this alloy contains a high density of screw dislocations which on annealing become converted into helices. At the copper end some XRDL work, especially on stacking fault probabilities, has been carried out by Christian and Spreadborough [6]. After these initial studies, many improvements in theory and experimentation have taken place. One remarkable advance

in analytical techniques has been the method of moments initiated by Wilson [7, 8] and developed among others by Mitra [9, 10].

In the course of the present work, dislocation densities and fault probabilities in two single-phase alloys containing copper and aluminium – one at the copper end containing 5.87 wt% Al while the other is at the aluminium end containing 0.08 wt% Cu – and the two double-phase (α and θ) alloys Al-4 and 10 wt% Cu have been studied by the methods of moments.

2. Comments on the XRDL techniques used

Techniques used widely for XRDL studied include (i) the method of Williamson and Hall [11] based on the integral width of the line profile introduced by Laue [12], and (ii) the method of Warren and Averbach [13] based on the Fourier transform of the line profile. Although both these methods are very widely used, they depend on assumptions regarding the nature of the line profile. While the method of integral widths is based on the nature of the diffraction profiles for particle size as well as defect, the method of Fourier coefficients depend on assumptions regarding the strain profile only. No assumption regarding the particle size profile is necessary. Averbach and Warren [14] have assumed the strain profile to be of the Gaussian type, while Williamson and Smallman [15]

have assumed it to be of Cauchy type. Recently Langford [16] has assumed the strain distribution to be of the Voigt type and Wang and Yu [1] have made use of this assumption. However, there appears to be no *a priori* reason why any of the assumptions will be valid although all are equally plausible. There is no experimental method of verifying the correctness of either of the assumptions. Moreover, Mitra and Chaudhury [17] have pointed out some basic limitations of the method of the Fourier analysis of the line profiles.

However, all these uncertainties can be eliminated if one uses the method of moments developed by Wilson [7, 8] and Mitra [9, 10]. This method is independent of any assumption regarding the nature of the convoluting profiles. Hence, in the present investigation this method has been used.

3. Theoretical basis of the experimental technique

3.1. Determination of particle size and strain

We know that the variance or the second central moment about the mean of a distribution $h(x)$ is given by

$$W_h = \frac{\int_{-\alpha}^{+\alpha} x^2 [h(x) - \langle h \rangle] dx}{\int_{-\alpha}^{+\alpha} h(x) dx}$$

where $\langle h \rangle = \int xh(x) dx / \int h(x) dx$ is the mean or the first moment of the distribution.

Both $\langle h \rangle$ and W_h have the unique property that if $h(x)$ is a result of the convolution of n distributions $h_1(x), h_2(x), \dots, h_n(x)$, then whatever be the nature of these distributions the resultant first and second moment about the mean of the component convoluted profiles will be the algebraic sum of the corresponding moments of the component profiles, i.e.

$$\langle h \rangle = \langle h_1 \rangle + \langle h_2 \rangle + \langle h_3 \rangle + \dots + \langle h_n \rangle$$

and

$$W_h = W_{h_1} + W_{h_2} + W_{h_3} + \dots + W_{h_n}$$

Here

$$h(x) = h_1(x) * h_2(x) * h_3(x) * h_n(x)$$

where the asterisk represents a convolution.

Hence, if a line profile $I(S)$ has component profiles due to particle size $P(S)$ and a defect profile $D(S)$ i.e. if $H(S) = P(S) * D(S)$, then

$$W_h = W_p + W_D \quad (1)$$

irrespective of the natures of $P(S)$ and $D(S)$. This is also true for the geometrical profiles $G(S)$ and the pure diffraction profile $H(S)$, so that

$$I(S) = H(S) * G(S)$$

and

$$W_I = W_h + G_h \quad (2)$$

The variance of the line profile can be corrected for geometrical and instrumental effects with the help of Equation 2 and that for the pure diffraction line profile can be separated into particle size and other defect parametric contributions with the help of Equation 1 once the explicit analytic forms of W_p and

W_D are known. Mitra [10] has derived the equation

$$\frac{W_h \cos \theta}{\lambda \sigma} = \frac{1}{2\pi^2 p} + \frac{n^2 \lambda}{\sigma \cos \theta} \frac{\langle S^2 \rangle}{a^2} \quad (3)$$

where W_h = the variance of the observed diffraction profile corrected for geometrical and instrumental broadenings, θ = Bragg angle corresponding to the reflection under study, λ = wavelength of the radiation used, σ = angular range of the reflection under study, p = average effective particle size, $\langle S^2 \rangle$ = average squared effective strains, n = the order of the reflection and a = lattice spacing corresponding to reflection.

Mitra [10] has shown that a plot of $W_h \cos \theta / \lambda \sigma$ against $n^2 \lambda / \sigma \cos \theta$ is linear with an intercept of $1/2\pi^2 p$ on the $W_h \cos \theta / \lambda \sigma$ axis and a slope of $\tan^{-1} (\langle S^2 \rangle / a^2)$ from which $1/p$ and $\langle S^2 \rangle$ can be obtained. It has been shown by Warren [18] that for fcc crystals

$$\frac{1}{p} = \frac{1}{T} + \frac{1.5\alpha + \beta}{aI(a+b)} \sum_l |L_0| \quad (4)$$

where T is the true particle size of the microcrystallinities, α and β are respectively the stacking and twinning fault probabilities, $L_0 = h + k + l$ where h, k, l are the Miller indices of the reflection studied and a, b are components of L_0 which are unbroadened and broadened by faults, respectively. Equation 4 as derived by Warren [18] is valid when the apparent particle size p is calculated from

$$\left. \frac{dA_p(t)}{dt} \right|_{t \rightarrow 0} = -\frac{1}{p}$$

where $A_p(t)$ is the t th order Fourier transformation of $P(S)$.

For the case of determination of particle size by the method of variance, Wilson [7] showed that

$$W = -\frac{\sigma}{2\pi^2} \left[\frac{A'_p(0)}{A_p(0)} \right]$$

in reciprocal lattice units, which when converted to (2θ) units becomes identical with the first term of Equation 3. Here

$$A_p(0) = 1 \quad \text{and} \quad A'_p(0) = \left. \frac{dA_p(t)}{dt} \right|_{t=0}$$

which is the same as the Warren [18] expression for $1/p$. Thus $1/p$ determined by the method of second moments has the same significance as $1/p$ as determined by Warren [18]. In Equation 4, $\alpha = \alpha' - \alpha''$ where α' is the intrinsic and α'' the extrinsic stacking fault probabilities [19]. Having obtained p from a graphical solution of Equation 3 by the method described by Mitra [10], T can be determined with the help of Equation 4 once α, β and $[1/I(a+b)] \sum_l |L_0|$ are known. Values of $[1/I(a+b)] \sum_l |L_0|$ are given by Warren [18] for different reflections (h, k, l values) of fcc and bcc lattices. α and β are determined in the way described below.

3.2. Determination of the stacking-fault parameter α

The method for studying the stacking-fault parameter α used in the course of these investigations is due to

Warren and Warekois [20], who showed that the combined peak shift of the (1 1 1) and (2 0 0) reflections of an fcc crystal due to stacking fault α is given by

$$\begin{aligned} & \Delta(2\theta_{200} - 2\theta_{111}) \\ &= -\frac{45\sqrt{3}}{2\pi^2} \alpha [2 \tan \theta_{200} + \tan \theta_{111}] \quad (5) \end{aligned}$$

where $2\theta_{200}$ and $2\theta_{111}$ are the peak shifts of (2 0 0) and (1 1 1) reflections, measured in terms of the angle of scattering in degrees. $\Delta(2\theta_{200} - 2\theta_{111})$ has been obtained from

$$\begin{aligned} & (2\theta_{200} - 2\theta_{111})_{\text{cold-worked}} - (2\theta_{200} - 2\theta_{111})_{\text{annealed}} \\ &= \Delta(2\theta_{200} - 2\theta_{111}) \end{aligned}$$

3.3. Determination of β

Wagner [21] showed that

$$\frac{\langle h \rangle_{111} - \langle h \rangle_{200}}{11 \tan \theta_{111} + 14.6 \tan \theta_{200}} = \beta + 4.5\alpha'' \quad (6)$$

Here $\langle h \rangle_{111}$ and $\langle h \rangle_{200}$ represent the first moment of the intensity profile in (2 θ) units of the 1 1 1 and 2 0 0 reflections of an fcc crystal. The profiles are supposed to have been corrected for the Lorentz-polarization factor.

4. Experimental technique

The samples studied are the alloys containing copper and aluminium and of the following compositions

- (i) 99.92 wt % Al, 0.08 wt % Cu
- (ii) 96 wt % Al, 4 wt % Cu
- (iii) 90 wt % Al, 10 wt % Cu
- (iv) 5.87 wt % Al, 94.13 wt % Cu

Spectroscopically pure aluminium and copper rods supplied by Johnson Matthey, London, were used for preparing the alloys. The alloys after homogenization were cold-drawn and then filed at room temperature (30°C). The filings were then studied at different stages of annealing by crystal-monochromatized radiation from an X-ray generator running at 30 kV and 20 mA. X-rays diffracted at various angles were measured by a Geiger counter followed by an electronic circuit panel and chart recorder. Initially, the chart was run at the rate of 1/4° min⁻¹ to locate the positions and width of the reflections. Then for actual analysis the Geiger counter detector was moved manually so that the time for 10 000 counts at each position was noted and the statistical error in counting came down to the order of 1%. Full details of the experimental arrangements have been described by Mitra [22]. The line profiles were corrected for geometrical broadening by the Stokes [23] deconvolution technique. Pure instrumental broadening for aluminium-rich alloys was obtained from spectroscopically pure aluminium filings annealed at 500°C for 4 h, and that for the copper-rich sample was obtained from spectroscopically pure copper filings annealed at 800°C for 8 h. Each intensity profile was now corrected for background scattering by the method due to Mitra and Misra [24], for temperature diffused scattering by the method of Chipman and Paskin [25] and for defect

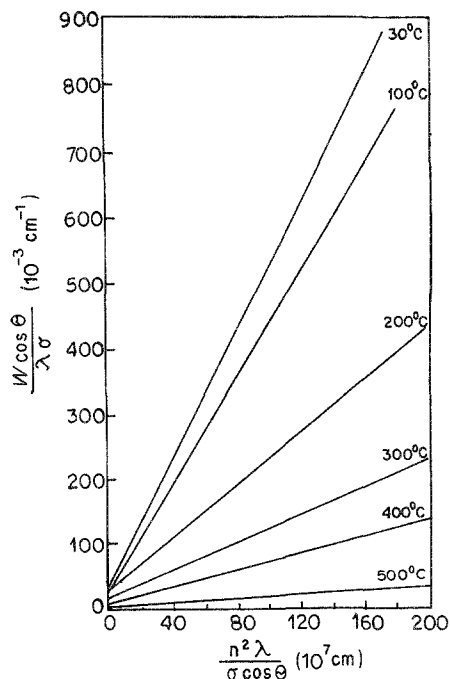


Figure 1 Determination of particle size and strain by the method of variance from the plot of $W \cos \theta / \lambda \sigma$ against $n^2 \lambda / \sigma \cos \theta$ for the alloy Cu-5.87 wt % Al. (1 1 1) directions.

diffused scattering by the method of Borie [26]. The reflections were finally corrected for extinction by the method of Mitra *et al.* [27].

Having obtained the profiles of the reflections and corrected them as above for various factors, the parameters $\langle h \rangle$ and W were obtained for all of them with the range of integration σ varying within permissible limits [28]. Next, by using Equation 3, the effective particle size and the root mean squared strain $\langle S^2 \rangle^{1/2}$ were determined. Corrections for non-additivity and curvature terms were made as advocated by Mitra and Mukherjee [29]. One set of the relevant linear plots (for Cu-5.87% Al) is shown in Fig. 1. The stacking fault probability α and twinning fault probability β were determined with the help of Equations 5 and 6. For evaluation of α , a Guinier asymmetric quartz monochromator was used which achieved a sufficient separation between $\text{Cu}K_{\alpha_1}$ and $\text{Cu}K_{\alpha_2}$ lines, so that the latter radiation was dispensed with and the measurement was carried out with only $\text{Cu}K_{\alpha_1}$ radiation. Solving Equations 4, 5 and 6 the values of T , α' , α'' and β have been obtained. The values of α' , α'' , β and D_{\min} are shown in Table I. D_{\min} is calculated by using the expression $D_{\min} = 0.82 / (2.31 / 2P_{111} - 1 / P_{200})$.

5. Discussion

5.1. Effect of the solute atom

In the course of the present investigations, the samples studied have been four alloys containing aluminium and copper. Two of these alloys, namely Al-0.08 wt % Cu and Cu-5.87 wt % Al, have a single phase each. The two double-phase alloys are Al-4 and 10% Cu. It will be interesting to compare the different physical parameters measured in the course of these investigations and hence try to observe the influence of atoms of one kind on the lattice of others. The comparative study of the different parameters has been described below.

TABLE I Calculated values of stacking and twinning fault probabilities and minimum stacking fault width

Sample	Temperature of annealing (°C)	Stacking fault probability		Twinning fault probability, $\beta \times 10^3$	Minimum stacking-fault width, D_{\min} (nm)
		Intrinsic, $\alpha' \times 10^3$	Extrinsic, $\alpha'' \times 10^{-3}$		
Al-0.08% Cu	30	3.4	0	8.2	88.5
	100	1.8	0	4.3	124.3
	200	0	0	0	158.2
	300	0	0	0	290.7
Al-4% Cu	30	36	4	48	9.6
	100	28	3	37	15.8
	200	12	2	25	18.4
	300	5	1	23	38.6
	400	2	0	23	62.9
Al-10% Cu	30	37	4	51	12.9
	100	30	3	42	11.3
	200	14	2	31	29.3
	300	7	1	29	28.6
	400	3	0	26	41.3
Cu-5.87% Al	30	32	3	65	22.6
	100	20	2	42	22.6
	200	8.5	1.1	31	22.6
	300	4.3	0.8	12	23.9
	400	0	0	0	29.7
	500	0	0	0	47.4

5.2. Hardness

Table II shows that the effect of addition of 0.08 wt % Cu to aluminium is to increase its VPN hardness at the cold-worked stage to a much greater extent than at the annealed state. The hardness of super-pure aluminium cold-worked to greater than 99.9% is about 30 VPN, while that of the alloy Al-0.08 wt % Cu similarly cold-worked is 56 VPN, i.e. about double the former value. The hardness of the cold-worked sample of aluminium comes down to 20 VPN on annealing at 300°C for half an hour. The hardening of the alloy Al-0.08 wt % Cu comes down on the other hand to the value 29 VPN on similar heat treatment. Thus, the addition of 0.08 wt % Cu to aluminium does not

increase the hardness of the annealed sample but increases its work-hardenability to a much greater extent. Similar results are obtained for the case of addition of 5.87 wt % Al to copper. While the hardnesses of the alloy and copper, similarly cold-worked, are 210 and 125 VPN, respectively, those of the samples annealed at 500°C for half an hour are 79 and 51 VPN, respectively. It is also evident that an increase in the proportion of the solute atoms tends to increase the hardness of the cold-worked sample, as is evident from the values of hardnesses of aluminium alloys containing 0.08, 4 and 10 wt % Cu. The increase in hardness of the two-phase alloys indicates the influence of the precipitation of the θ -phase.

TABLE II Hardness of four copper-aluminium alloys

Sample	Temperature of annealing (°C)	Hardness (VPN)
Al-0.08% Cu	30	56
	100	54
	200	45
	300	29
Al-4% Cu	30	78
	100	75
	200	67
	300	56
	400	34
Al-10% Cu	30	132
	100	128
	200	85
	300	52
	400	35
Cu-5.87% Al	30	210
	100	195
	200	172
	300	98
	400	86
	500	79

5.3. Dislocation density and stored energy

Figs 2 and 3 show the dislocation density and the stored energy of the samples under study at different stages of annealing. The dislocation density has been evaluated from the equation

$$\rho_p = 3n/T^2$$

where T is the particle size. It assumes that each crystallite face is the starting point of n dislocation lines, each of which terminates at the opposite surface. n is generally unity but often it may be that $n > 1$. This consideration does not take into account the Frank-Read sources of dislocations which may eventually contribute to the strain. The correlation between dislocation density and hardness is quite remarkable. For materials and annealing stages at which the dislocation density is high, the hardness of the material is also correspondingly high. This shows that hardness is enhanced by the pinning of dislocations by solute atoms.

The stored energy has been calculated with the help of the expression derived by Faulkner [30] and given

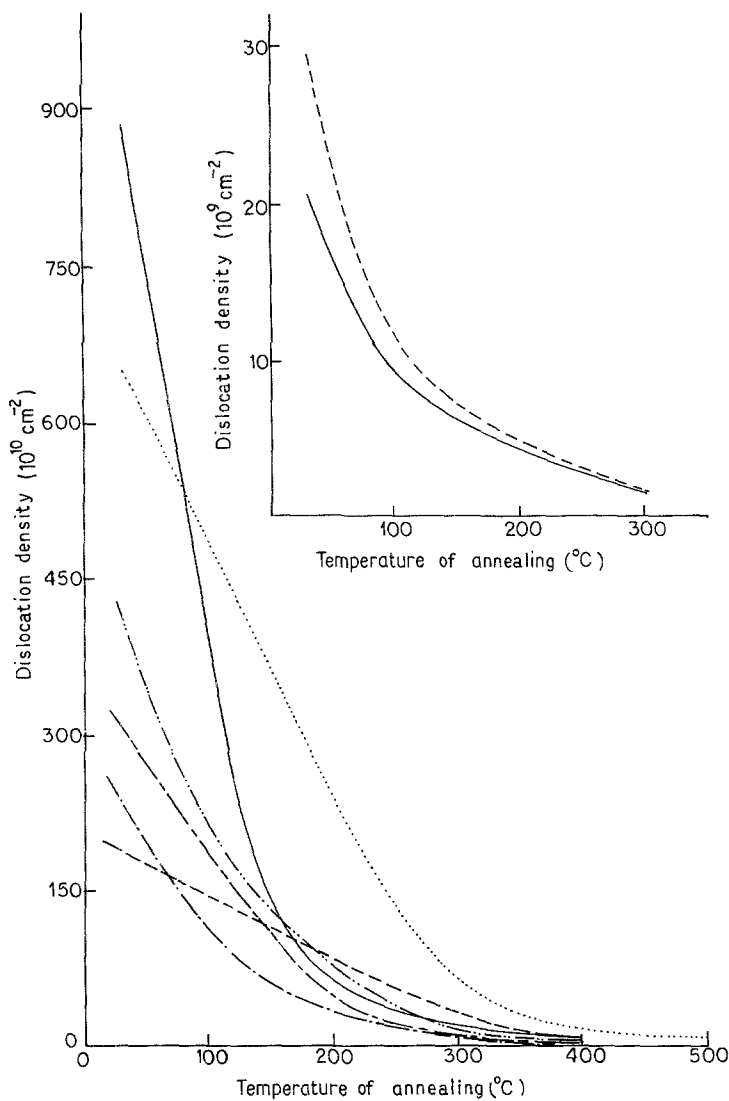


Figure 2 Plot of dislocation density against temperature of annealing. Main plot: (---) Al-4% Cu, (111) direction; (-.-.) Al-4% Cu, (100); (---) Al-10% Cu, (111); (—) Al-10% Cu, (100); (---) Cu-5.87% Al, (111); (-.-.) Cu-5.87% Al, (100). Inset: (—) Al-0.08% Cu, (111); (---) Al-0.08% Cu, (100).

as

$$v = \frac{15E}{2(3 - 4\nu + 8\nu^2)} \langle S^2 \rangle$$

where v is the energy stored per unit volume of the material, E its Young's modulus, ν is the Poisson's ratio and $\langle S^2 \rangle$ is the average squared strain as in Equation 3. E has been evaluated along different directions from the values of elastic constants determined by the method due to Giri and Mitra [31]. The value of ν is 0.34 [32] for both copper and aluminium and hence the values of v for alloys too have been taken to be 0.34. The results of the calculations are shown in Fig. 3. Since the energy stored in the crystallites of the material is principally due to the dislocations in it, it is natural to expect that the nature of the variation of the dislocation density will be similar to that of the variation of the stored energy in it. That this is so is quite evident from a comparison of the two sets of graphs shown in Figs 2 and 3. It is observed that the stored energy is a maximum for the (111) plane of the alloy Cu-5.87% Al. The diameter of the aluminium atom being 0.2856 nm, when the aluminium atoms are placed substitutionally in a copper lattice - copper atoms have diameters of 0.2585 nm each - a large strain is developed, the copper atoms are all pushed around and a large amount of potential energy is stored in the alloy. On the other hand, when copper

atoms with a smaller diameter are pushed inside an aluminium matrix, the solute atoms are fitted in with relative ease and only the formation of the θ phase takes place.

5.4. Relation between particle size and strain
Rovinskii and Rybakova [33] and Despujols and Warren [34] have observed an inverse relation between particle size and strain. To determine whether this relationship is also valid for the values measured in the course of the present investigation, the strain values determined by the method of variance have been plotted against the corresponding particle size values. Fig. 4 shows this plot. The resulting curves are approximately rectangular hyperbolae. Thus the inverse relation is found to be valid for the present case too. An explanation may be given in the following way. The dislocation densities determined from the particle size T and r.m.s. strain $\langle S^2 \rangle^{1/2}$ are ρ_T and ρ_s , respectively, and are given by [35]

$$\rho_T = \frac{3n}{T^2} \quad (7)$$

and

$$\rho_s = \frac{K \langle S^2 \rangle}{F b^2} \quad (8)$$

where n is the number of dislocations per particle face,

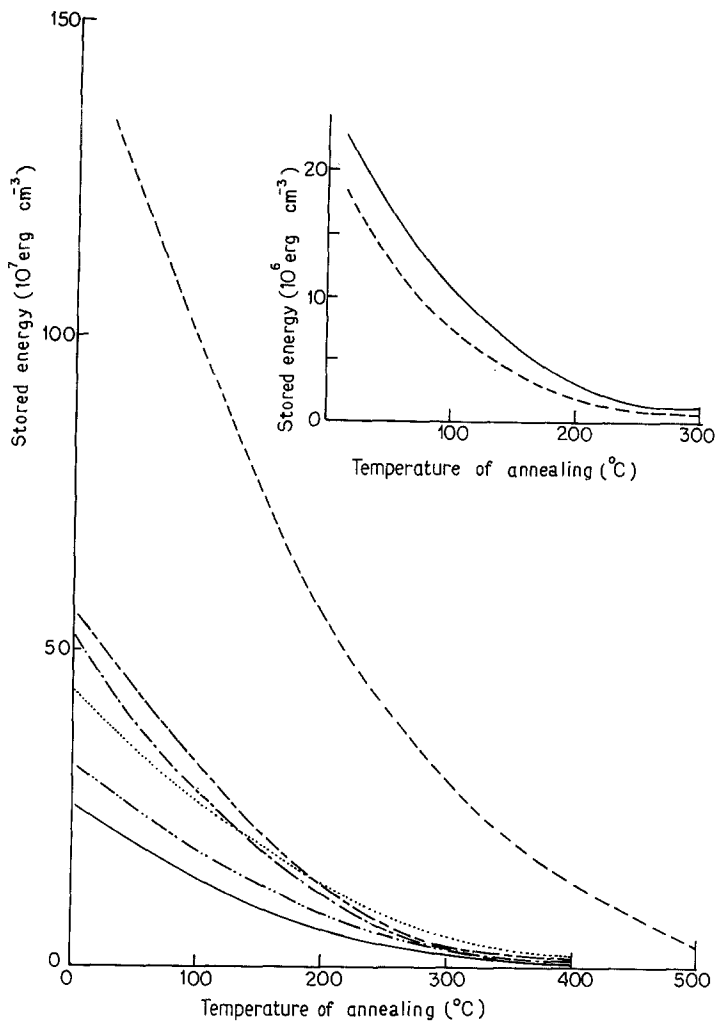


Figure 3 Plot of stored energy against temperature of annealing. Main plot: (---) Al-4% Cu, (111) direction; (---) Al-4% Cu, (100); (—) Al-10% Cu, (111); (---) Al-10% Cu, (100); (---) Cu-5.87% Al, (111); (···) Cu-5.87% Al, (100). Inset: (—) Al-0.08% Cu, (111); (---) Al-0.08% Cu, (100).

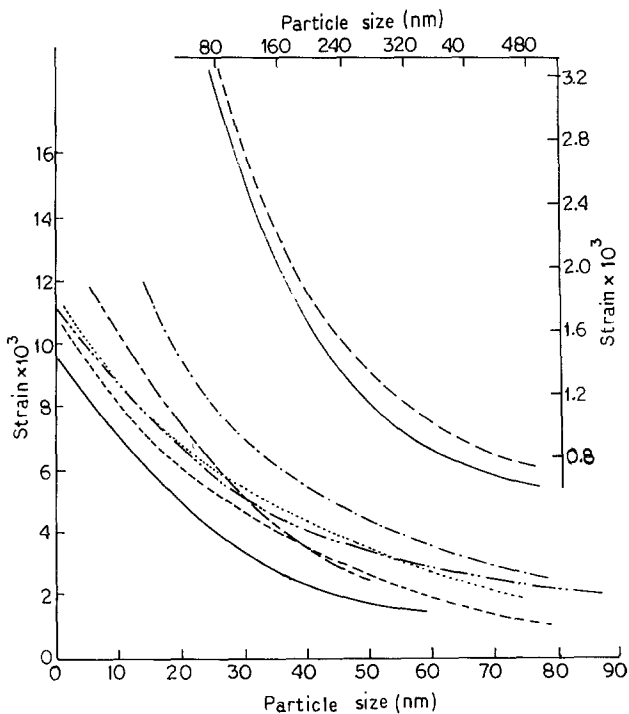


Figure 4 Plot of particle size against strain. Main plot: (---) Al-4% Cu, (111) direction; (---) Al-4% Cu, (100); (—) Al-10% Cu, (111); (---) Al-10% Cu, (100); (---) Cu-5.87% Al, (111); (···) Cu-5.87% Al, (100). Inset: (—) Al-0.08% Cu, (111); (---) Al-0.08% Cu, (100).

b is the Burgers vector, $K = 6\pi E/\mu \ln(r/r_0)$ and $F = V/V_c$; V = energy per dislocation taking into account effects of interactions, V_c = energy per isolated dislocations, E and μ are the Young's and rigidity modulus, respectively, r the radius of the crystal containing the dislocations and r_0 a suitably chosen integration limit, usually about 10^{-7} cm. Generally $q_T \neq q_s$, but they are most likely to be related through a sample factor. If m be such a factor, then

$$\frac{3n}{T^2} = m \frac{K \langle S^2 \rangle}{F b^2}$$

$$\langle S^2 \rangle^{1/2} T = \left(\frac{3nF}{mK} \right)^{1/2} b \quad (9)$$

F and K are generally constant quantities for a given substance and a given type of dislocation; so are m and b , and if n is kept constant, $\langle S^2 \rangle^{1/2} T$ will also be constant. Based on this result, a hypothesis regarding the growth of particle size may be that n for a given type of dislocation and substance is fixed irrespective of dislocation density. As with annealing, the number of dislocations decreases and the remaining dislocations are spread evenly over a larger area than previously, so that the number of dislocations per particle face is kept constant. This results in enlargements of the particle faces and hence of the particle size.

5.5. Stacking and growth faults and stacking fault widths

Table I shows the effect of annealing on extrinsic and intrinsic fault probabilities and of growth faults as well as the minimum width of stacking-fault ribbons in the cases of the alloys studied. It is noteworthy that while growth faults are extensively and persistently present, stacking faults are relatively rare and are eliminated with relative ease. The extrinsic fault probabilities are much lower compared to the intrinsic fault probabilities. The intrinsic fault probabilities are probably due to the blow-up of vacancies, while the extrinsic faults are due to the pinning down of dislocations by foreign atoms. The gradual merger of the CuAl_2 phases disintegrating from the matrix of the θ phase causes the gradual disappearance of the α'' parameter. The α parameters are due to rearrangement of point defects accompanied by their creation and annihilation, but leading to their final disappearance. The minimum widths of stacking-fault ribbons also decrease, and at complete annealing they finally vanish.

Acknowledgements

The authors avail themselves of this opportunity to thank the Council of Scientific and Industrial Research, New Delhi, for financial help which enabled them to carry out this work. They also thank the authorities of the Indian Association for the Cultivation of Science, Calcutta for providing facilities to carry out this work.

References

1. S. WANG and W. YU, *J. Mater. Sci. Lett.* **4** (1985) 635.
2. A. SATO, Y. SUGISAKI and T. MORI, *Phil. Mag.* **A51** (1985) 133.
3. A. GUINER, *Ann. Phys.* **18** (1939) 161.
4. G. D. PRESTON, *Nature* **172** (1939) 116.
5. G. THOMAS and J. WASHBURN, "Electron Microscopy and Strength of Crystals" (InterScience, New York, 1963).
6. J. CHRISTIAN and J. SPREADBOROUGH, *Phil. Mag.* **1** (1956) 1069.
7. A. J. C. WILSON, *Proc. Phys. Soc.* **80** (1962) 286.
8. *Idem, ibid.* **81** (1963) 41.
9. G. B. MITRA, *Br. J. Appl. Phys.* **15** (1964) 917.
10. *Idem, Acta Crystallogr.* **17** (1964) 765.
11. G. K. WILLIAMSON and W. H. HALL, *Acta Metall.* **1** (1953) 22.
12. M. V. LAUE, *Z. Krist.* **64** (1926) 115.
13. B. E. WARREN and B. L. AVERBACH, *J. Appl. Phys.* **21** (1950) 595.
14. B. L. AVERBACH and B. E. WARREN, *ibid.* **20** (1949) 1066.
15. G. K. WILLIAMSON and R. E. SMALLMAN, *Acta Crystallogr.* **7** (1954) 574.
16. J. I. LANGFORD, *J. Appl. Crystallogr.* **11** (1978) 10.
17. G. B. MITRA and A. K. CHAUDHURY, *ibid.* **7** (1974) 350.
18. B. E. WARREN, *J. Appl. Phys.* **32** (1961) 2428.
19. H. HOLLOWAY and M. S. KLAUKINS, *ibid.* **40** (1969) 1681.
20. B. E. WARREN and E. P. WAREKOIS, *Acta Metall.* **3** (1955) 473.
21. C. N. J. WAGNER, *Acta Metall.* **5** (1957) 427, 477.
22. G. B. MITRA, *Br. J. Appl. Phys.* **16** (1965) 77.
23. A. R. STOKES, *Proc. Phys. Soc.* **61** (1948) 382.
24. G. B. MITRA and N. K. MISRA, *Br. J. Appl. Phys.* **17** (1966) 1319.
25. D. R. CHIPMAN and A. PASKIN, *J. Appl. Phys.* **30** (1959) 1992.
26. B. S. BORIE, *Acta Crystallogr.* **9** (1956) 617.
27. G. B. MITRA, B. K. MATHUR and B. K. SAMANTARAY, *Indian J. Phys.* **53A** (1979) 148.
28. G. B. MITRA and P. S. MUKHERJEE, *ibid.* **56A** (1982) 175.
29. *Idem, J. Appl. Crystallogr.* **14** (1981) 421.
30. E. A. FAULKNER, *Phil. Mag.* **5** (1960) 519.
31. A. K. GIRI and G. B. MITRA, *J. Mater. Sci. Lett.* in press.
32. M. P. TOSI, "Solid State Physics", Vol. 16 edited by F. Seitz and D. Turnbull (Academic, New York) p. 292.
33. B. M. ROVINSKII and L. RYBAKOVA, *Izv. Acad. Nauk. SSSR Ser. Tekhn.* **10** (1952) 1483.
34. J. DESPUJOLS and B. E. WARREN, *J. Appl. Phys.* **29** (1958) 195.
35. G. K. WILLIAMSON and R. E. SMALLMAN, *Phil. Mag.* **1** (1956) 34.

Received 28 May
and accepted 22 August 1986